Park, Kang-Wook; Lee, Jun-Whan; Jeong, Woo-Chang; Cho, Yong-Sik

Observation and Numerical Prediction of 2011 East Japan Tsunami Inpacific Ocean

OBSERVATION AND NUMERICAL PREDICTION OF 2011 EAST JAPAN TSUNAMI IN PACIFIC OCEAN

Kang-Wook Park[1], Jun-Whan Lee[2], Woo-Chang Jeong[3], Yong-Sik Cho[4]

ABSTRACT

A numerical simulation of transoceanic propagation of tsunamis is conducted by solving the linear shallow-water equations with the leap-frog in the staggered grid system. When a tsunami propagates a long distance, the dispersion effects may play an important role and should be considered in numerical simulation. Recently, Cho *et al.* (2007) developed a practical dispersion-correction scheme to consider the dispersion effects by adjusting the numerical dispersion. The developed scheme is verified by comparing numerical results with available analytical solution. In this study, the propagation of the East Japan Tsunami occurred on March 2011 is simulated and predicted free surface profiles are compared with measurements at DART buoys. The LSWE with dispersion-correction scheme model results, such as the arrival time and the leading wave elevation at tidal stations, are more agreeable than the LSWE model with the observed data recorded at several DART buoys.

1. INTRODUCTION

The East Japan Tsunami that occurred in March, 2011 was one of the most destructive tsunamis in the history. The epicenter of 2011 East Japan Earthquake was located about 70 kilometers east of the Oshika Peninsula of Tohoku Province, Japan. The earthquake triggered large tsunamis reaching heights of up to 40.5 meters at Miyako, Iwate Prefecture, and invaded up to 10 km inland in the Sendai area. After the tsunami generation, it is very important to predict changes of water level as early as possible by using a numerical simulation.

In this study, the propagation of the East Japan Tsunami is simulated across Pacific Ocean considering frequency dispersion effects on the actual terrain. First, the governing equations are described to investigate transoceanic propagation of tsunamis. The numerical model is then employed to simulate propagation of 2011 East Japan Tsunami. Obtained numerical results such as the arrival time and the leading wave crest elevation at tidal stations are compared with available observed data. A detailed analysis is conducted. The dispersion effects can be significant for

[1] Graduate Student, Department of Civil and Environmental Engineering, Hanyang University, 17 Haengdang-dong, Seongdong-gu, Seoul 133-791, Korea (kangwogi@hanyang.ac.kr)
[2] Graduate Student, Department of Civil and Environmental Engineering, Hanyang University, 17 Haengdang-dong, Seongdong-gu, Seoul 133-791, Korea (junwhan89@hanyang.ac.kr)
[3] Assistant Professor, Department of Civil Engineering, Kyungnam University, 11 Woryeong-dong, Masanhappo-gu, Changwon-si, Gyeongsangnam-do, 631-701, Korea (jeongwc@kyungnam.ac.kr)
[4] Corresponding Author, Professor, Department of Civil and Environmental Engineering, Hanyang University, 17 Haengdang-dong, Seongdong-gu, Seoul 133-791, Korea (ysc59@hanyang.ac.kr)

amplitude estimation in transoceanic propagation of tsunamis. Finally, summary of the study and concluding remarks will be described.

2. GOVERNING EQUATIONS

The linear shallow-water equations were used in most of the previous studies due to numerical difficulty of using the linear Boussinesq equations. The linear shallow-water equations have an advantage that they can use a relatively simple numerical scheme such as the leap-frog finite difference scheme. The linear shallow-water equations are derived from the linear Boussinesq equations by eliminating the frequency dispersion term in the momentum equations. The linear shallow-water equations can be written in the following form (Liu *et al*., 1994).

$$\frac{\partial \zeta}{\partial t}+\frac{\partial P}{\partial x}+\frac{\partial Q}{\partial y}=0 \tag{1}$$

$$\frac{\partial P}{\partial t}+gh\frac{\partial \zeta}{\partial x}=0 \tag{2}$$

$$\frac{\partial Q}{\partial t}+gh\frac{\partial \zeta}{\partial y}=0 \tag{3}$$

where ζ is the free surface displacement, h is the still water depth, and P and Q are the depth-averaged volume fluxes in the $x-$ and $y-$axis directions, respectively, and g is the acceleration due to gravity. But, the linear shallow-water equations do not have frequency dispersion terms. So, Cho *et al*. (2007) have developed practical dispersion-correction scheme to consider frequency dispersion by using numerical dispersion.

3. NUMERICAL SCHEME

The numerical schemes proposed by Imamura and Goto (1988) and Cho and Yoon (1998) are summarized briefly and a new scheme is then proposed. Imamura and Goto used a leap-frog finite difference scheme to discretize in a staggered grid system.

Cho *et al.* (2007) modified Imamura and Goto's scheme to mimic the frequency dispersion with the numerical dispersion caused by finite difference approximation. The scheme followed as

$$\frac{\zeta_{i+1/2,j}^{n+1/2}-\zeta_{i,j}^{n-1/2}}{\Delta t}+\frac{P_{i+1/2,j}^{n}-P_{i-1/2,j}^{n}}{\Delta x}+\frac{Q_{i,j+1/2}^{n}-Q_{i,j-1/2}^{n}}{\Delta y}=0 \tag{4}$$

$$\begin{aligned}&\frac{P_{i+1/2,j}^{n+1}-P_{i+1/2,j}^{n}}{\Delta t}+gh_{i+1/2,j}\frac{\zeta_{i+1,j}^{n+1/2}-\zeta_{i,j}^{n+1/2}}{\Delta x}+\frac{\alpha}{12\Delta x}gh_{i+1/2,j}\left[\zeta_{i+2,j}^{n+1/2}-3\zeta_{i+1,j}^{n+1/2}+3\zeta_{i,j}^{n+1/2}-\zeta_{i-1,j}^{n+1/2}\right]\\&+\frac{\gamma}{12\Delta x}gh_{i+1/2,j}\left[\left(\zeta_{i+1,j+1}^{n+1/2}-2\zeta_{i+1,j}^{n+1/2}+\zeta_{i+1,j-1}^{n+1/2}\right)-\left(\zeta_{i,j+1}^{n+1/2}-2\zeta_{i,j}^{n+1/2}+\zeta_{i,j-1}^{n+1/2}\right)\right]=0\end{aligned} \tag{5}$$

$$\begin{aligned}&\frac{Q_{i,j+1/2}^{n+1}-Q_{i,j+1/2}^{n}}{\Delta t}+gh_{i,j+1/2}\frac{\zeta_{i,j+1}^{n+1/2}-\zeta_{i,j}^{n+1/2}}{\Delta x}+\frac{\alpha}{12\Delta y}gh_{i,j+1/2}\left[\zeta_{i,j+2}^{n+1/2}-3\zeta_{i,j+1}^{n+1/2}+3\zeta_{i,j}^{n+1/2}-\zeta_{i,j-1}^{n+1/2}\right]\\&+\frac{\gamma}{12\Delta y}gh_{i,j+1/2}\left[\left(\zeta_{i+1,j+1}^{n+1/2}-2\zeta_{i,j+1}^{n+1/2}+\zeta_{i-1,j+1}^{n+1/2}\right)-\left(\zeta_{i+1,j}^{n+1/2}-2\zeta_{i,j}^{n+1/2}+\zeta_{i-1,j}^{n+1/2}\right)\right]=0\end{aligned} \tag{6}$$

The variables (ζ, P and Q) are defined in the previous section. Indices (i, j) and n denote spatial nodes and the time level, respectively. The spatial grid sizes in the $x-$ and $y-$ axis directions are represented by Δx and Δy, respectively, and the time step size is symbolized by Δt.

In eqs. 5 and 6, the dispersion–correction factors, α and γ, are determined by a relation of depth, spatial grid size and time step size. If both α and γ are zero, eqs. 4-6 are reduced to Imamura and Goto's scheme. If α and γ become zero and one, respectively, eqs. 4-6 are reduced to Cho and Yoon's scheme.

The numerical dispersion generated by the proposed scheme is investigated. Following the approach suggested by Warming and Hyett (1974), the Taylor series expansions of variables ζ, P and Q at a point represented by (n, i, j) are applied to eqs. 4-6. To derive a modified equation, all the higher time derivatives are replaced by the corresponding spatial derivatives and the volume flux components, P and Q, are eliminated. After lengthy algebra a modified equation for ζ is obtained as

$$\frac{\partial^2\zeta}{\partial t}-C_0^2\left(\frac{\partial^2\zeta}{\partial x^2}+\frac{\partial^2\zeta}{\partial y^2}\right)-C_0^2\frac{(\Delta x)^2}{12}(1+\alpha-C_r^2)\times\left(\frac{\partial^4\zeta}{\partial x^4}+\frac{\partial^4\zeta}{\partial y^2\partial x^2}+\frac{\partial^4\zeta}{\partial y^4}\right)$$
$$+(1+\alpha-\gamma)C_0^2\frac{(\Delta x)^2}{6}\frac{\partial^4\zeta}{\partial x^2\partial y^2}=O((\Delta x)^3,(\Delta x)^2\Delta t,(\Delta t)^2\Delta x,(\Delta t)^3) \tag{7}$$

in which a uniform grid, $\Delta x=\Delta y$, is used, and $C_0\left(=\sqrt{gh}\right)$ and $C_r\left(=C_0\Delta t/\Delta x\right)$ represent the phase velocity of a linear shallow-water wave and the Courant number, respectively. The leading order terms in eq. 7 are the same as those in the wave equation. The terms of $O\left((\Delta x)^2\right)$ and of higher order are the results of numerical discretization. Comparing eq. 7 with the linear Boussinesq equation, these equations are seen to be identical as long as the following relations are satisfied. That is,

$$\alpha=\frac{4h^2+gh(\Delta t)^2-(\Delta x)^2}{(\Delta x)^2},\quad \gamma=\alpha+1 \tag{8}$$

4. CASE STUDY - 2011 EAST JAPAN TSUNAMI

4.1 Initial Condition

The initial free surface displacement of tsunamis caused by an undersea movement is very difficult. The parameters of the undersea earthquake used to determine the initial free surface displacement are listed in Table 1. The detailed description of the determination of initial free surface displacement can be found in Mansinha and Smylie (1971).

Table 1 Fault parameters for 2011 East Japan Tsunami.

	Latitude ($^\circ N$)	Longitude ($^\circ E$)	Depth (km)	Length (km)	Width (km)	Strike ($^\circ$)	Dip ($^\circ$)	Rake ($^\circ$)	Slip (m)
Value 1	38.80	144.00	5.1	186	129	203	16	101	24.7
Value 2	37.33	142.80	17.0	194	88	203	15	83	6.1

The initial free surface displacement is shown in Figure 1. The maximum free surface displacement is 11.0m at the right side of the north fault.

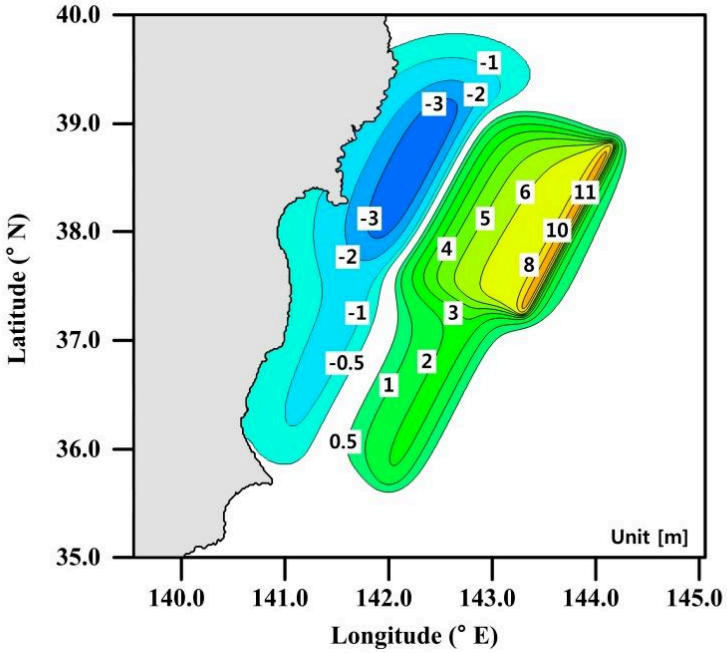

Figure 1 Initial free surface displacement profile of 2011 East Japan Earthquake.

4.2 Bathymetric Data and Grid System

The bathymetric data of the Pacific Ocean is generated from ETOPO1. ETOPO1 is a gridded data set of the land and seafloor elevations of the whole Earth. The grid size is 1min of latitude and longitude in the ETOPO1. And the grid system is designed to simulate the transoceanic propagation of 2011 East Japan Tsunami and presented in Table 2.

Table 2 Grid system for numerical simulation.

Upper right coordinate	Lower left coordinate	Grid size	Mesh number	Time step size
$65^\circ N$ $135.0^\circ W$	$0^\circ N$ $140.0^\circ E$	1 min (≒1850 m)	5098 x 3898	2.66 sec

4.3 Comparison of Observed data and Simulated Results

Free surface profiles of 2011 East Japan Tsunami are recorded at many DART buoys operating in the northern Pacific, and are considered the signals at buoys of 21418, 21413, 21419, 21415, 21414, 46408, 46402 and 46403 (Figure 2).

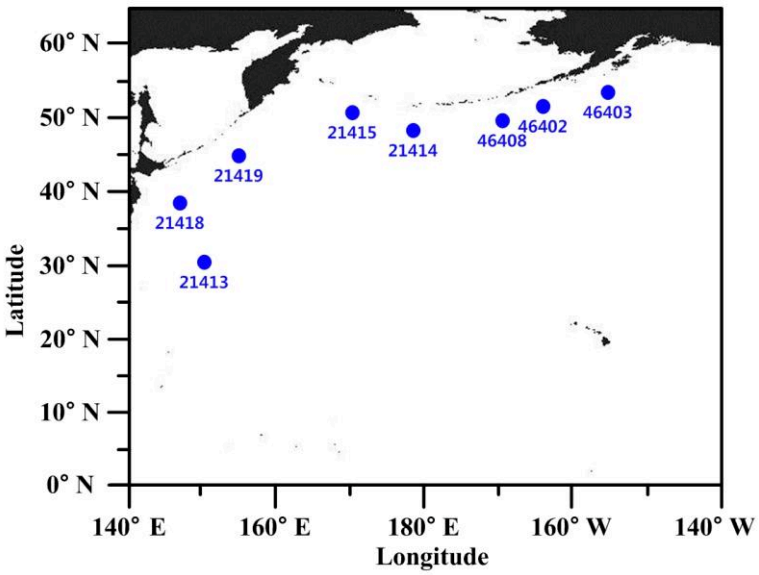

Figure 2 Computational region and location of DART buoys.

The numerical simulation was run for 12 hours of tsunami propagation, in order for waves to reach the most distant DART buoys. Figure 3 and Figure 4 represented simulated results (LSWE: blue dotted line, LSWE with dispersion-correction scheme: red line) comparing with observed data (green line). In general, the first wave of tsunamis is important in predicting the damage. Thus, the leading wave crest elevation and the arrival time are focused.

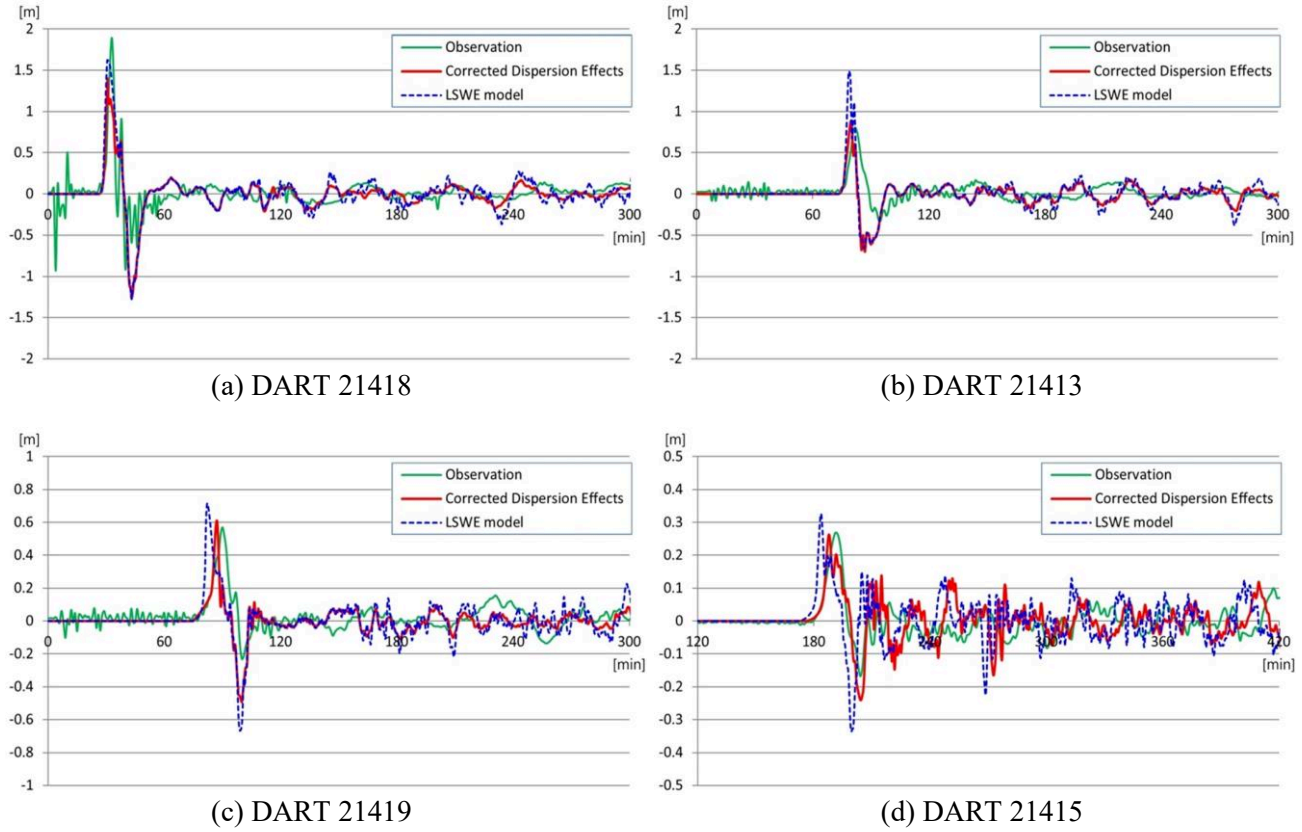

(a) DART 21418 (b) DART 21413

(c) DART 21419 (d) DART 21415

Figure 3 Comparisons of water level at DART 21418, 21413, 21419, 21415 obtained by Observation, LSWE and LSWE with dispersion-correction scheme model.

Figure 3 shows temporal variation of the free surface obtained by LSWE model and LSWE with dispersion-correction scheme model at locations of DART buoys given in Figure 2. As shown in these figures, LSWE with dispersion-correction scheme model results agree well with observations, especially the leading wave crest elevation and the arrival time. As we move away from the epicenter (Figure 4), the simulation results consistently underpredict the leading wave elevation (3~5cm) at each location. And the simulation results predict that the wave arrives slightly sooner (2~6min) than seen in observations. These can be explained in part by a combination of grid and bathymetric resolution effects, as well as slight errors in the source location and triggering. Additional systematic errors on propagation times could results from the fact that the Earth is not perfectly spherical.

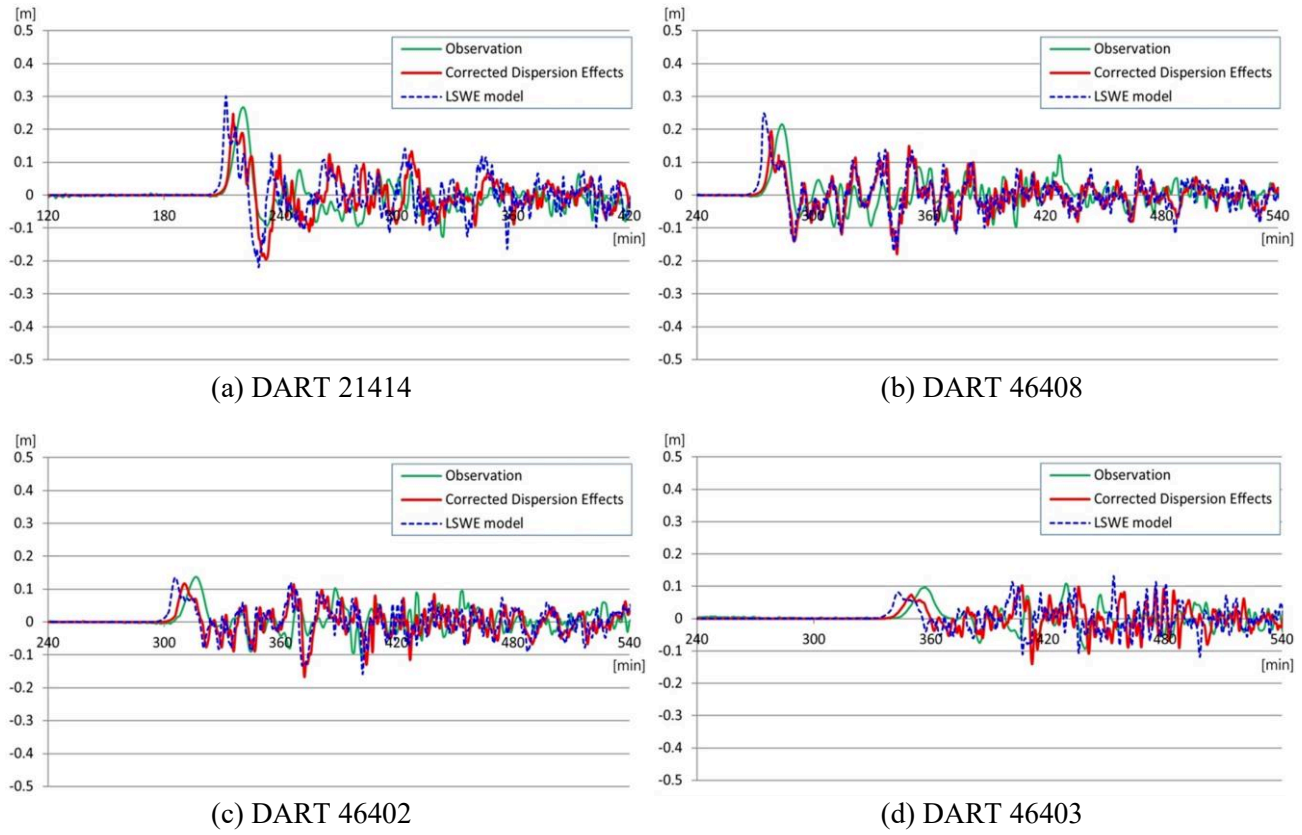

(a) DART 21414 (b) DART 46408

(c) DART 46402 (d) DART 46403

Figure 4 Comparisons of water level at DART 21414, 46408, 46402, 46403 obtained by Observation, LSWE and LSWE with dispersion-correction scheme model.

Overall, results for the LSWE with dispersion-correction scheme model agree well with DART buoy data. It is shown that the arrival time and the leading wave crest elevation are obtained accurately. As a result, frequency dispersion effects can be significant for amplitude estimation in transoceanic tsunami propagation.

Figure 5 shows wave patterns at time 1 hour using LSWE and LSWE with dispersion-correction scheme methods. Due to the dispersion effects the LSWE with dispersion-correction scheme model shows a series of unbroken wave behind the leading wave, therefore, wave patterns are significantly different from that of LSWE model. From the LSWE with dispersion-correction scheme model result, it is seen that length of the wave train in the eastern region is longer than in the western region(close to Japan). As eqs. 5, 6 and 8 suggest the magnitude of the dispersive term is proportional to the water depth. Therefore, the dispersion effect in the eastern region is stronger than that in the western region. Additionally, the dispersion effect in the eastern region is enhanced through the longer distance of propagation.

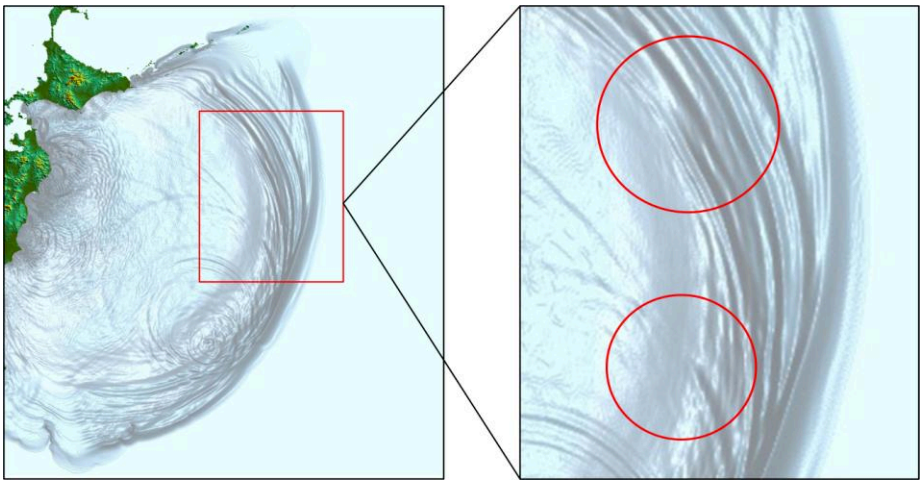

(a) LSWE model result

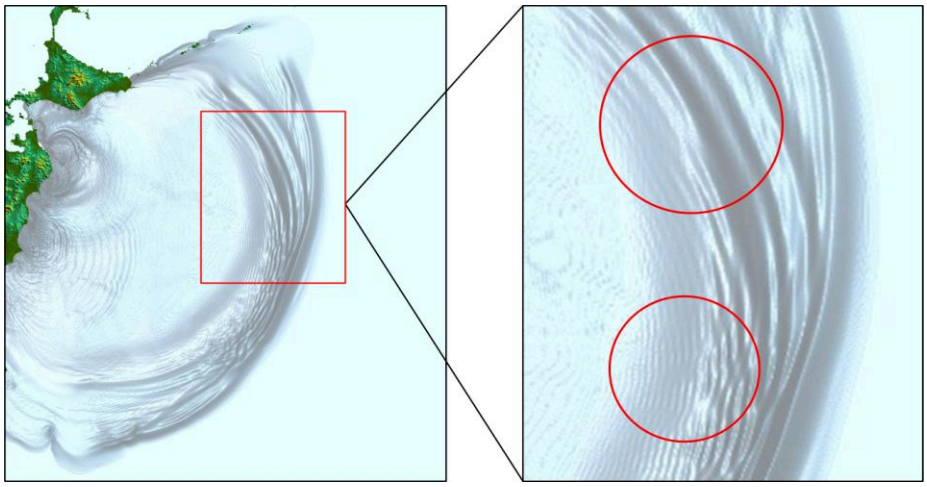

(b) LSWE with dispersion-correction scheme model result

Figure 5 Comparison of water surface computed at 1hour from the onset of the earthquake

5. CONCLUDING REMARKS

The linear Boussinesq equations including the Coriolis force may be adequate to describe the propagation of transoceanic tsunamis. However, the linear Boussinesq equations may require a small mesh size to suppress the numerical dispersion, and consume a huge computer memory space and excessive computational time to deal with frequency dispersion terms expressed by third order derivatives. Therefore, solving the linear Boussinesq equations directly may not be an economical approach for simulating the distant propagation of tsunamis. A finite difference numerical model that can consider the dispersion effects is being developed by using the linear shallow-water equations instead of the linear Boussinesq equations. Thus, a numerical simulation of a far field tsunami is performed by the numerical model proposed by Cho *et al.* (2007).

In this study, the target event is 2011 East Japan Tsunami. The numerical model is employed to simulate the transoceanic tsunami in Pacific Ocean. The LSWE with dispersion-correction scheme model results, such as the arrival time and the leading wave elevation at tidal stations, are more agreeable than the LSWE model with the observed data recorded at several DART buoys.

ACKNOWLEDGEMENTS

This work was supported by the National Research Foundation of Korea (NRF) grant funded by the Korea government(MEST) (No. 2011-0015386).

REFERENCES

Cho, Y.-S. and Yoon, S.B. (1998) "A Modified Leap-Frog Scheme for Linear Shallow-Water Equations", Coastal Engineering Journal, Vol. 40, No. 2, pp. 191-205.

Cho, Y.-S., Sohn, D.-H. and Lee, S.-O. (2007) "Practical Modified Scheme of Linear Shallow-Water Equations for Distant Propagation of Tsunamis", Ocean Engineering, Vol. 34, No. 11-12, pp. 1769-1777.

Kajiura, K. and Shuto, N. (1990) Tsunami, in the sea, edited by B. Le Mehaute. and D.M. Hanes., Vol. 9, Part B, John Wiley & Sons, pp. 395-420.

Liu, P.L.-F., Cho, Y.-S., Yoon, S.B. and Seo, S.N. (1994) Numerical Simulations of the 1960 Chilean Tsunami Propagation and Inundation at Hilo, Hawaii, in Recent Development in Tsunami Research, edited by M. I. El-Sabh, Kluwer Academic Publishers, pp. 99-115.

Mansinha, L., Smylie, D.E. (1971) "The Displacement Fields of Inclined Faults", Bull. Seismol. Soc. Am. Vol. 61, No. 5, pp. 1433-1440.

Imamura, F., Shuto, N. and Goto, C. (1988) "Numerical Simulations of the Transoceanic Propagation of Tsunamis", Proceedings of 6th Congress Asian and Pacific Regional Division, IAHR, Japan, pp. 265-272.

Warming, R.F., Hyett, B.J. (1974) "The Modified Equation Approach to the Stability and Accuracy Analysis of Finite Difference Methods", Journal of Computational Physics, Vol. 14, pp. 159-179.

Yoon, S.B. (2002) "Propagation of Distant Tsunamis over Slowly Varying Topography", Journal of Geophysical Research, Vol. 107, No. 10, pp. 4(1) -4(11).